Molecular Biology of the Cell
Vol. 16, 5480–5492, December 2005

The Oxysterol-binding Protein Homologue ORP1L Interacts with Rab7 and Alters Functional Properties of Late Endocytic Compartments

Marie Johansson,* Markku Lehto,* Kimmo Tanhuanpää,† Timothy L. Cover,‡ and Vesa M. Olkkonen*

*Department of Molecular Medicine, National Public Health Institute, FI-00251 Helsinki, Finland; †Light Microscopy Unit, Institute of Biotechnology, FI-00014 University of Helsinki, Finland; and ‡Division of Infectious Diseases, Vanderbilt University School of Medicine and Veterans Affairs Medical Center, Nashville, TN 37232

Submitted March 7, 2005; Revised July 28, 2005; Accepted September 8, 2005
Monitoring Editor: Jean Gruenberg

ORP1L is a member of the human oxysterol-binding protein (OSBP) family. ORP1L localizes to late endosomes (LEs)/lysosomes, colocalizing with the GTPases Rab7 and Rab9 and lysosome-associated membrane protein-1. We demonstrate that ORP1L interacts physically with Rab7, preferentially with its GTP-bound form, and provide evidence that ORP1L stabilizes GTP-bound Rab7 on LEs/lysosomes. The Rab7-binding determinant is mapped to the ankyrin repeat (ANK) region of ORP1L. The pleckstrin homology domain (PHD) of ORP1L binds phosphoinositides with low affinity and specificity. ORP1L ANK- and ANK+PHD fragments induce perinuclear clustering of LE/lysosomes. This is dependent on an intact microtubule network and a functional dynein/dynactin motor complex. The dominant inhibitory Rab7 mutant T22N reverses the LE clustering, suggesting that the effect is dependent on active Rab7. Transport of fluorescent dextran to LEs is inhibited by overexpression of ORP1L. Overexpression of ORP1L, and in particular the N-terminal fragments of ORP1L, inhibits vacuolation of LE caused by *Helicobacter pylori* toxin VacA, a process also involving Rab7. The present study demonstrates that ORP1L binds to Rab7, modifies its functional cycle, and can interfere with LE/lysosome organization and endocytic membrane trafficking. This is the first report of a direct connection between the OSBP-related protein family and the Rab GTPases.

INTRODUCTION

The cytosolic oxysterol-binding protein OSBP was identified in the 1980s (Taylor *et al*., 1984; Taylor and Kandutsch, 1985), and a role for the protein in cholesterol and sphingomyelin metabolism has been implicated previously (Lagace *et al*., 1997, 1999). Families of proteins homologous to OSBP have recently been identified in eukaryotic organisms from yeast to human (Lehto and Olkkonen, 2003). These proteins, denoted as OSBP-related proteins (ORPs), have been implicated in diverse aspects of cellular physiology, including sterol and phospholipid metabolism, vesicle transport, cell signaling, and cell cycle control. The mechanism by which ORP proteins contribute to these processes has, however, remained largely enigmatic. The ORP gene products are cytosolic but associate peripherally with distinct subcellular membrane compartments. The human ORP family consists of 12 members that can be divided into six subfamilies (Jaworski *et al*., 2001; Lehto *et al*., 2001). These proteins have a unique OSBP-related ligand-binding domain (ORD) in their C-terminal half and an N-terminal portion that contains a pleckstrin homology domain (PHD). In OSBP, the PHD, which binds several phosphoinositides, was shown to mediate targeting of the protein to Golgi membranes (Levine and Munro, 1998; Lagace *et al*., 1999; Levine and Munro, 2002). Another membrane-targeting determinant, with the consensus sequence EFFDAxE, was recently identified in eight human ORPs and a number of other proteins involved in lipid metabolism. This motif mediates interaction with vesicle-associated membrane protein-associated proteins, integral membrane proteins of the endoplasmic reticulum (Loewen *et al*., 2003).

ORP1 is present in human tissues as two major variants, ORP1L and ORP1S. In addition to the ORD present in ORP1S, ORP1L has an N-terminal extension with three ankyrin (ANK) repeats, motifs commonly involved in protein–protein interactions (Sedgwick and Smerdon, 1999; Johansson *et al*., 2003). We have previously shown that ORP1L localizes to late endosomes and has the capacity to modulate the transactivation potential of liver X receptors, whereas the cytosolic ORP1S shows no such effect (Johansson *et al*., 2003). Late endosomes (LEs) are multifunctional organelles that receive internalized cargo and receptors destined for degradation from early/sorting endosomes and a variety of molecules such as components of the lysosomal hydrolytic apparatus from the *trans*-Golgi network. The LEs communicate with lysosomes to deliver their cargo to this degradative end

This article was published online ahead of print in *MBC in Press* (http://www.molbiolcell.org/cgi/doi/10.1091/mbc.E05–03–0189) on September 21, 2005.

Address correspondence to: Vesa M. Olkkonen (vesa.olkkonen@ktl.fi).

Abbreviations used: ANK, ankyrin repeat; FRAP, fluorescence recovery after photobleaching; LE, late endosome; ORD, oxysterol-binding protein-related ligand-binding domain; ORP, oxysterol-binding protein-related protein; OSBP, oxysterol-binding protein; PHD, pleckstrin homology domain.

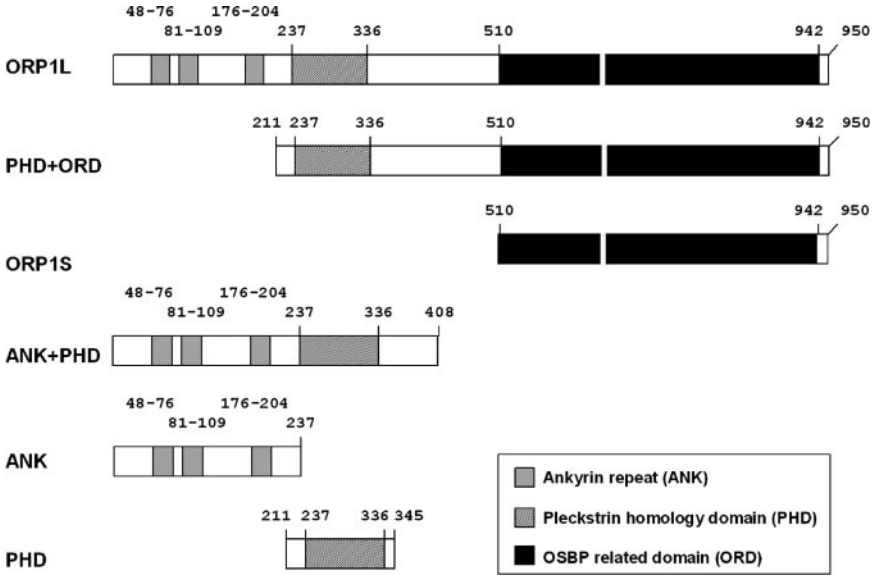

Figure 1. Schematic presentation of the ORP1L constructs used. The numbers indicate amino acid residues.

station, but they also sort and recycle various molecules, including receptors that are returned to the *trans*-Golgi (Bishop, 2003; Maxfield and McGraw, 2004). The small Rab GTPases are master regulators of intracellular membrane trafficking events, and they are found at specific locations on membrane organelles that constitute the biosynthetic and endocytic pathways of eukaryotic cells (Pfeffer, 2001; Zerial and McBride, 2001). The GTPase Rab7 is present on LEs and lysosomes (Chavrier *et al*., 1990; Meresse *et al*., 1995) and controls membrane trafficking between early and late endosomes and from LEs to lysosomes (Feng *et al*., 1995; Press *et al*., 1998). Rab7 also regulates the microtubule-dependent motility of late endocytic compartments (Cantalupo *et al*., 2001; Jordens *et al*., 2001; Lebrand *et al*., 2002; Harrison *et al*., 2003). In addition, Rab7 has been connected to a variety of LE functions, such as cellular vacuolization induced by *Helicobacter pylori* (Papini *et al*., 1997; Li *et al*., 2004), intracellular replication of *Salmonella* (Guignot *et al*., 2004; Harrison *et al*., 2004; Marsman *et al*., 2004), maturation of phagosomes (Harrison *et al*., 2003; Vieira *et al*., 2003; Ng Yan Hing *et al*., 2004), formation of autophagic vacuoles (Gutierrez *et al*., 2004; Jager *et al*., 2004), internalization/degradation of nutrient receptors (Edinger *et al*., 2003), and cholesterol and sphingolipid egress from LEs (Choudhury *et al*., 2002). Mutations of the Rab7 gene in humans have been identified as the cause of ulcero-mutilating neuropathy (Verhoeven *et al*., 2003; Houlden *et al*., 2004).

In the present study, we analyze the late endosomal targeting of ORP1L. The protein is shown to interact via its ankyrin repeat region with Rab7, leading to modification of the Rab7 functional cycle, and via its PHD with phosphoinositide lipids. Furthermore, functional effects of the overexpression of ORP1L or its truncated fragments on late endosome/lysosome morphology and endocytic membrane trafficking are investigated.

MATERIALS AND METHODS

Cell Culture and Transfection

HeLa cells were grown in DMEM (Sigma-Aldrich, St. Louis, MO), 10% fetal bovine serum (FBS), 20 mM HEPES, 100 U/ml penicillin, and 100 μg/ml streptomycin. Cells were transiently transfected for 24–36 h with cDNA constructs in complete medium using LipofectAMINE 2000 (Invitrogen, Carlsbad, CA). COS-1 cells were grown in the same medium, but transfection was carried out using FuGENE 6 transfection reagent (Roche Diagnostics, Indianapolis, IN). Transfections were carried out according to the manufacturers' instructions.

cDNA Constructs and Vectors

The ORP1L cDNA fragments are described in Johansson *et al*. (2003). ORP1L cDNA encodes the full-length ORP1L protein (aa 1–950). Truncated fragments comprising different functional elements of ORP1L were generated (Figure 1). Inserts were subcloned into mammalian pcDNA4HisMax expression vectors (Invitrogen), pcDNA3.1 (Invitrogen), or pEGFP-C (BD Biosciences Clontech, Palo Alto, CA). For production of glutathione *S*-transferase (GST) fusion proteins, inserts were subcloned into pGex-1λT or pGex4T-1 (GE Healthcare, Little Chalfont, Buckinghamshire, United Kingdom).

For the luciferase two-hybrid assay, ORP1L cDNA was cloned into a vector derived from pM (BD Biosciences Clontech), pM2 (Dr. Ivan Sadowski, Department of Biochemistry and Molecular Biology, Faculty of Medicine, Vancouver, British Columbia, Canada). The pG5luc and the pSV-β-Galactosidase vectors were from Promega (Madison, WI).

pEGFP-Rab5 and pEGFP-Rab9 expression constructs were kindly provided by Dr. Marino Zerial (Max Planck Institute for Molecular Cell Biology and Genetics, Dresden, Germany) and pEGFP-Rab7 by Dr. Angela Wandinger-Ness (Department of Pathology, University of New Mexico Health Sciences Center, Albuquerque, NM). The pEGFP-p50dynamitin construct is described in Marsman *et al*. (2004). For the luciferase two-hybrid assay, wild-type Rab7 was subcloned into vector pVP16 (BD Biosciences Clontech) and used as template for generation of the constitutively active Q67L and the dominant negative T22N mutants, using the QuikChange site-directed mutagenesis kit (Stratagene, La Jolla, CA).

Antibodies

A GST-ORP1 fusion protein corresponding to amino acids 428–950 in ORP1L was used for raising the R250 antibody, which reacts with both ORP1S and ORP1L (Johansson *et al*., 2003). The ORP1L-specific antibody R247 was raised against a GST fusion protein containing amino acids 428–553 of ORP1L. This N-terminal region comprises the ankyrin repeats in ORP1L. The ORP1 antiserum (1:5 dilution in phosphate-buffered saline [PBS]) was preadsorbed with glutathione-Sepharose 4B (GE Healthcare) carrying GST. The unbound fraction was incubated with a cyanogen bromide-activated Sepharose 4B column to which the antigen fragment had been coupled. The antibodies were eluted with 0.2 M glycine, pH 2.8, neutralized, and dialyzed against PBS or PBS, 50% glycerol.

The chicken anti-Rab7 antibody (Stein *et al*., 2003; Dong *et al*., 2004) was a kind gift from Dr. Angela Wandinger-Ness, and rabbit anti-Rab7 was purchased from Santa Cruz Biotechnology (Santa Cruz, CA). Mouse monoclonal antibody (mAb) against the Xpress epitope was from Invitrogen, monoclonal lysosome-associated membrane protein-1 (Lamp-1) (H4A3) antibody was from Santa Cruz Biotechnology, and anti-p150^{glued} was from BD Biosciences (San Jose, CA).

Production of GST Fusion Proteins

GST fusion proteins were produced from plasmids pGEX4T1-Rab7, pGEX1λT-ORP1PHD, and phospholipase Cδ (PLCδ) PHD in pGEX1λT. The

PLCδ PHD cDNA was a kind gift from Dr. Tamas Balla (National Institutes of Health, Bethesda, MD). The proteins were expressed in *Escherichia coli* DH5α (Invitrogen) and purified using glutathione-Sepharose 4B (GE Healthcare) according to the manufacturer's protocol. The Rab7 fusion protein was in PBS, 2 mM $MgCl_2$, and 1 mM dithiothreitol (DTT) during all handling steps.

Immunofluorescence Microscopy

Transfected cells were fixed with 4% paraformaldehyde (PFA), 250 mM HEPES, pH 7.4, for 30 min and permeabilized for 25 min with 0.05% Triton X-100 in PBS. In tetramethylrhodamine (TRITC)-dextran (Invitrogen) endocytosis experiments, cells were fixed with PFA/lysine/periodate fixative (2% PFA, 75 mM lysine, 10 mM sodium periodate, and 0.0375 M phosphate buffer, pH 6.2) and permeabilized for 5 min with 0.05% Triton X-100 in PBS. In some experiments, cells were treated with 10 μM nocodazole for 30 min at 37°C before fixation. Nonspecific binding of antibodies was blocked with 10% FBS/phosphate-buffered saline for 30 min, after which cells were incubated with primary antibody in 5% FBS/phosphate-buffered saline for 30 min at 37°C. Bound primary antibodies were visualized with Alexa Fluor secondary antibody conjugates (Invitrogen). Cells were mounted in Mowiol (Calbiochem, San Diego, CA) containing 50 mg/ml 1,4-diazocyclo-[2,2,2]octane (Sigma-Aldrich). The specimens were analyzed with a TCS SP1 laser scanning confocal microscope (Leica, Wetzlar, Germany). TRITC-dextran fluorescence was quantified with pinhole open (airy 5) using a Leica TCS SP1 confocal microscope and the Quantify function of the Leica LCS software package.

Immunoprecipitation

HeLa cells seeded on 6-cm dishes were transfected for 24 h. Cells were washed twice with ice-cold PBS and 500 μl of lysis buffer (10 mM HEPES, pH 7.6, 150 mM NaCl, 0.5 mM $MgCl_2$, 10% glycerol, and 0.5% Triton-X 100) with complete EDTA-free protease inhibitor cocktail (Roche Diagnostics). Cells were scraped and kept on ice for 15 min and then centrifuged for 15 min at 13,000 rpm at 4°C. The supernatant was preabsorbed at 4°C for 30 min with 30 μl of protein G-Sepharose 4 Fast Flow (GE Healthcare). The recovered supernatant was incubated with ORP1L-, Xpress-, or control antibodies at 4°C overnight. The lysate–antibody mixture was added to fresh protein G-Sepharose and incubated at 4°C on a roller for 6 h. Beads were washed four times with lysis buffer and boiled in 30 μl of SDS-PAGE loading buffer. Proteins were resolved on 12.5% SDS-polyacrylamide gels and transferred to Hybond-C Extra nitrocellulose (GE Healthcare). Nonspecific binding of antibodies was blocked with, and all antibody incubations were carried out in 5% fat-free powdered milk in 10 mM Tris-HCl, pH 7.4, 150 mM NaCl, and 0.05% Tween 20. The bound antibodies were visualized with horseradish peroxidase-conjugated goat anti-rabbit or goat anti-mouse IgG (Bio-Rad, Hercules, CA) and the enhanced chemiluminescence system ECL (GE Healthcare). Immunoprecipitation of endogenous proteins was carried out in the same manner using 20 mM HEPES, pH 7.6, 150 mM NaCl, 2.0 mM $MgCl_2$, 10% glycerol, 0.5% Triton-X 100, and 1 mM DTT as lysis buffer.

Two-Hybrid Luciferase Assay

COS-1 cells seeded on 12-well plates were transfected for 24 h. Transfection mixtures consisted of 400 ng of wild-type (wt) or mutant pVP16-Rab7, 400 ng of pM2-ORP1L, 200 ng of pG5luc, and 100 ng of pSV-β-galactosidase. Empty pVP16 and pM2 vectors were used as controls. Mixtures were transfected in triplicate. Cells were washed twice with ice-cold PBS, and 100 μl of reporter lysis buffer (Promega) was added to each well. The lysates were centrifuged for 3 min at 13,000 rpm, and the supernatants were transferred to new tubes. For the luciferase activity assay, 20 μl of each supernatant was mixed with 100 μl of luciferase assay reagent (Promega), and the luminescence was measured using a Victor 1420 multilabel counter (PerkinElmer Wallac, Turku, Finland). For the β-galactosidase activity assay, 65 μl of reaction mixture consisting of 1 mM $MgCl_2$, 45 mM β-mercaptoethanol, 1 mg/ml ortho-nitrophenyl-β-D-galactopyranoside (Sigma-Aldrich), and 0.1 M Na-phosphate, pH 7.0, was mixed with 10 μl of lysate. Duplicate samples were incubated for 15–30 min at 37°C, and the reaction was stopped by adding 125 μl of 1 M Na_2CO_3. The absorbance was measured at 420 nm.

Pull-Down Assay of In Vitro-translated ORP1L Fragments

ORP1L fragments were translated in vitro using the TnT-coupled reticulocyte system (Promega) according to the manufacturer's instructions. Purified GST-Rab7 fusion protein (150 μg) or plain GST (150 μg) was bound to 30 μl of glutathione-Sepharose 4B in coupling buffer (PBS, 2 mM $MgCl_2$, and 1 mM DTT). Beads were washed once with coupling buffer and once with loading buffer (20 mM HEPES, 100 mM KAc, 0.5 mM $MgCl_2$, 1 mM DTT, and 2 mM EDTA, pH 7.2) and incubated with 10 μM guanosine 5′-*O*-(3-thio)triphosphate (GTPγS) in loading buffer for 1 h at 37°C. In vitro-translated fragments (12.5 μl), 10 mM $MgCl_2$, and 10 mg/ml albumin were added, and beads were incubated for 1 h at room temperature on a roller. The beads were washed three times with wash buffer (20 mM HEPES, 100 mM KAc, 5 mM $MgCl_2$, and 1 mM DTT, pH 7.2) and eluted with 30 μl of 15 mM glutathione in wash buffer for 20 min at room temperature. The supernatant was recovered and boiled in SDS-PAGE loading buffer. The samples were resolved in 12.5% or 15% SDS-polyacrylamide gels, which were fixed, incubated with Amplify (GE Healthcare), dried, and exposed on Kodak x-ray film at −70°C.

Fluorescence Recovery after Photobleaching (FRAP)

EGFP-Rab7 was expressed together with ORP1L or with empty pcDNA4HisMax vector (control) in HeLa cells grown on glass-bottomed microwell dishes (Mat-Tek, Ashland, MA). EGFP-Rab7 containing endo/lysosome clusters in the perinuclear region were photobleached at 488 nm. The long-range motility of these groups of organelles was negligible. FRAP experiments were performed on a Leica TCS-SP2 AOBS confocal microscope at 37°C under 5% CO_2 using a 63× numerical aperture 1.4 objective. A 6.5-μm^2 area was bleached with 100% of the argon laser power at 488 nm for 2.4 s. Fluorescence-recovery data were then acquired using low-intensity laser scanning. The intensity data were exported to Microsoft Excel and corrected for bleaching during recovery. The cells were thereafter fixed and processed for immunofluorescence microscopy using the Xpress antibody to verify expression of ORP1L in the double-transfected cells subjected to FRAP analysis.

Liposome Pull-Down Assay

The assay was adapted from the protocol of Schiavo *et al*. (1996). Liposomes were prepared by lyophilizing 297 nmol of egg-PC (Sigma-Aldrich), 0.03 μCi of [^{14}C]dipalmitoyl-phosphatidylcholine, and 3 nmol of butylated hydroxytoluene and 3 nmol of a specific phosphoinositide. Lipids were dissolved in 1 ml of sample buffer (20 mM HEPES-KOH and 100 mM KCl, pH 7.6) and sonicated at 7-μm amplitude (ZZMS-38121–114A tip) for 3 × 5 min with an MSE Soniprep 150 sonicator (Loughborough, United Kingdom). Liposomes were microcentrifuged for 15 min at 13,000 rpm, and the supernatant was recovered. The phosphoinositides phosphatidylinositol 3-phosphate, phosphatidylinositol 4-phosphate, and phosphatidylinositol 4,5-bisphosphate were from Matreya (Pleasant Gap, PA); phosphatidylinositol 5-phosphate, phosphatidylinositol 3,4-bisphosphate, phosphatidylinositol 3,5-bisphosphate, and phosphatidylinositol 3,4,5-trisphosphate were from Sigma-Aldrich. GST fusion proteins (50 μg) were bound to 30 μl of glutathione-Sepharose 4B beads (GE Healthcare) in PBS and washed twice with sample buffer. One-third of the respective liposome preparation was added to each protein-coupled Sepharose sample, and the beads were incubated for 30 min on a roller at room temperature. Samples were centrifuged at 500 × *g* for 2 min, and the supernatants were transferred into scintillation tubes. The beads were then washed three times with 500 μl of sample buffer, and each wash supernatant was transferred into scintillation tubes. The beads were collected into scintillation vials with 500 μl of sample buffer containing 1% SDS. OptiPhaseHiSafe 3 (PerkinElmer Wallac) was added, and radioactivity was measured using a WinSpectral 1414 liquid scintillation counter (PerkinElmer Wallac).

Tetramethylrhodamine-Dextran Uptake and Transport

pEGFP-ORP1L- or pEGFP-transfected HeLa cells were incubated at 37°C for 10 min with 5 mg/ml tetramethylrhodamine dextran mol. wt. 10,000 (Invitrogen) in serum-free medium. Cells were fixed immediately or after various chase times and analyzed as described in *Immunofluorescence Microscopy*.

VacA-induced Cell Vacuolation

VacA was purified from *H. pylori* strain 60190 as described previously (Cover *et al*., 1997). pEGFP-Rab7, along with either pcDNA4HisMax-ORP1L or pcDNA4HisMax-ANK+PHD expression constructs, were transfected into HeLa cells. VacA was activated by dropwise addition of 200 mM HCl until the pH was reduced to 3.0 (Cover *et al*., 1997, Li *et al*., 2004). Acid-activated VacA was diluted into culture medium containing 5 mM NH_4Cl to a final concentration of 5 μg/ml. Vacuolation was induced by incubating transfected cells in VacA-containing medium for 4 h. After incubation, cells were fixed, stained and analyzed as described in *Immunofluorescence Microscopy*.

RESULTS

ORP1L Colocalizes with Lamp-1 and Induces Abnormal LE Morphology

The subcellular localization of ORP1L in HeLa cells was studied by immunofluorescence microscopy. ORP1L was expressed in the cells by transient transfection, and images were acquired from cells with a moderate ORP1L expression level to avoid artifacts possibly caused by excessive overexpression of the protein. ORP1L localized on perinuclear membrane organelles that were positive for Lamp-1, thus representing late endocytic compartments (Figure 2, A–C). In most cells expressing ORP1L, abnormalities of LE/lysosome structure were evident. Clustering of the LE/lyso-

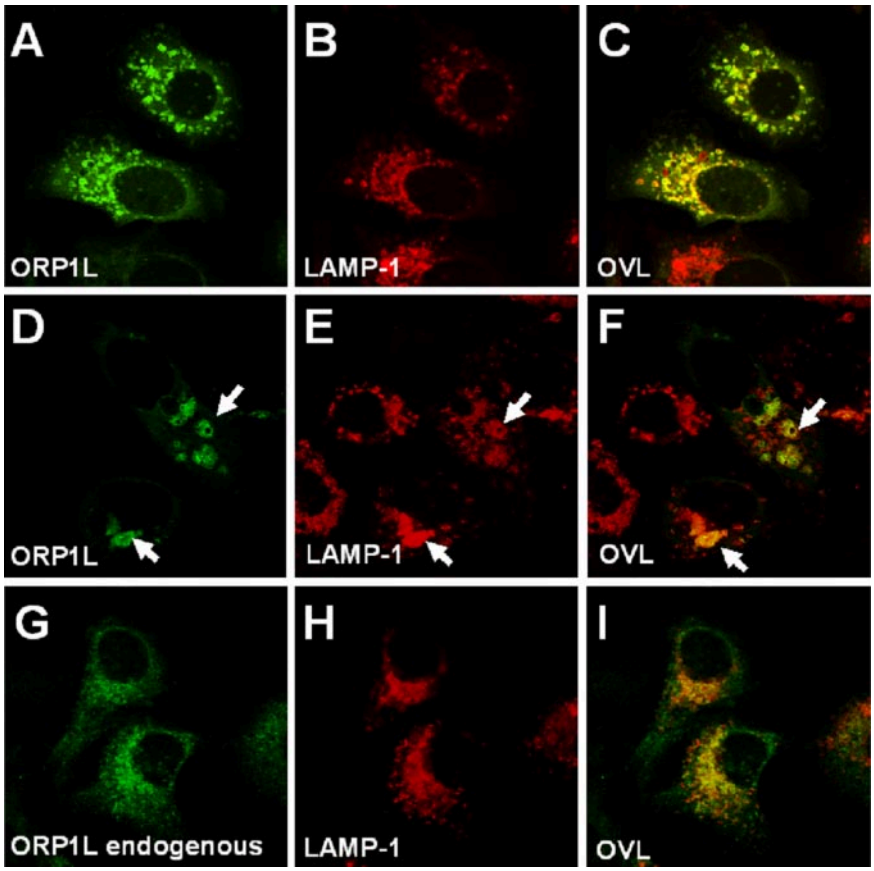

Figure 2. ORP1L colocalizes with Lamp-1 and its overexpression alters late endosome morphology in HeLa cells. Specimens were analyzed by confocal immunofluorescence microscopy. (A–C) Transfected cells overexpressing full-length human ORP1L. ORP1L and the endogenous Lamp-1 were visualized by specific rabbit (R247) and mouse monoclonal antibodies, respectively. (D–F) Transfected cells expressing ORP1L and displaying clustered and enlarged Lamp-1-positive compartments (indicated with arrows). (G–I) Endogenous ORP1L and Lamp-1 stained using the same antibodies. OVL, overlays.

somes was frequently observed, and some of the Lamp-1-positive compartments harboring expressed ORP1L were apparently enlarged (Figure 2, D–F).

The endogenous ORP1L in HeLa cells could be visualized using an affinity-purified antibody (R247) against the protein. The antibody stained vesicular structures in the perinuclear region that also colocalized with Lamp-1 (Figure 2, G–I), confirming that the protein expressed from the cDNA and the endogenous ORP1L have a similar subcellular distribution.

ORP1L Colocalizes with Rab7 and Rab9

The effects of ORP1L overexpression on LE/lysosome morphology suggested that the protein could be functionally connected with the machineries responsible for organelle motility, membrane tethering, docking, and fusion in the late endocytic pathway. Because the small Rab GTPases are central regulators of these events (Pfeffer, 2001; Zerial and McBride, 2001), we compared the localization of ORP1L to that of several Rab proteins. ORP1L and EGFP-Rab7 in transfected HeLa cells colocalized extensively as did the endogenous HeLa cell proteins (Figure 3, A–F). The localization pattern of the expressed ORP1L also overlapped extensively with another late endosomal GTPase, EGFP-Rab9 (Figure 3, G–I), whereas no colocalization was observed with EGFP-Rab5 (Figure 3, J–L) or EGFP-Rab6 (Figure 3, M–O).

ORP1L Interacts Physically with Rab7

Because interaction with Rab GTPase(s) seemed to be a potential mechanism for mediating the effects of ORP1L on LE/lysosome morphology, we carried out coimmunoprecipitation experiments. Untagged ORP1L was coexpressed in HeLa cells with Xpress epitope-tagged Rab7, Xpress epitope-tagged Rab9 (which both colocalize with ORP1L), or Xpress epitope-tagged Rab6 (no colocalization with ORP1L). Immunoprecipitations were performed with anti-Xpress or control antibodies, followed by Western blotting with anti-ORP1L. ORP1L was found to coprecipitate with Xpress-Rab7 from double-transfected cells, whereas no ORP1L protein was found in precipitates from double-transfected cells immunoprecipitated with an irrelevant control antibody or cells transfected with ORP1L alone precipitated with Xpress antibody (Figure 4A). Importantly, we were also able to demonstrate specific coimmunoprecipitation of the endogenous HeLa cell ORP1L with the endogenous Rab7, which was precipitated with a rabbit polyclonal antibody (Figure 4B). In experiments carried out using ORP1L and Xpress-tagged Rab9 or Rab6, no coprecipitation was detected, suggesting that the interaction observed is specific for Rab7 (Figure 4, C and D).

To obtain more evidence for an interaction between ORP1L and Rab7, we carried out two-hybrid experiments in COS cells. In these assays, we also tested the interaction of ORP1L with a GTPase deficient, constitutively active Rab7 Q67L and a dominant inhibitory-type mutant, T22N, which preferably binds GDP. Although significant luciferase activity was detected in cells cotransfected with ORP1L and either wt Rab7 or the Q67L mutant, the luciferase activity in cells cotransfected with the ORP1L and the Rab7 T22N mutant remained at the level of the empty vector (Figure 5). This provided further evidence for an interaction of ORP1L with Rab7 and suggested that ORP1L preferably interacts with active, GTP-bound Rab7. The result also indicates that the interaction between ORP1L and Rab7 is direct.

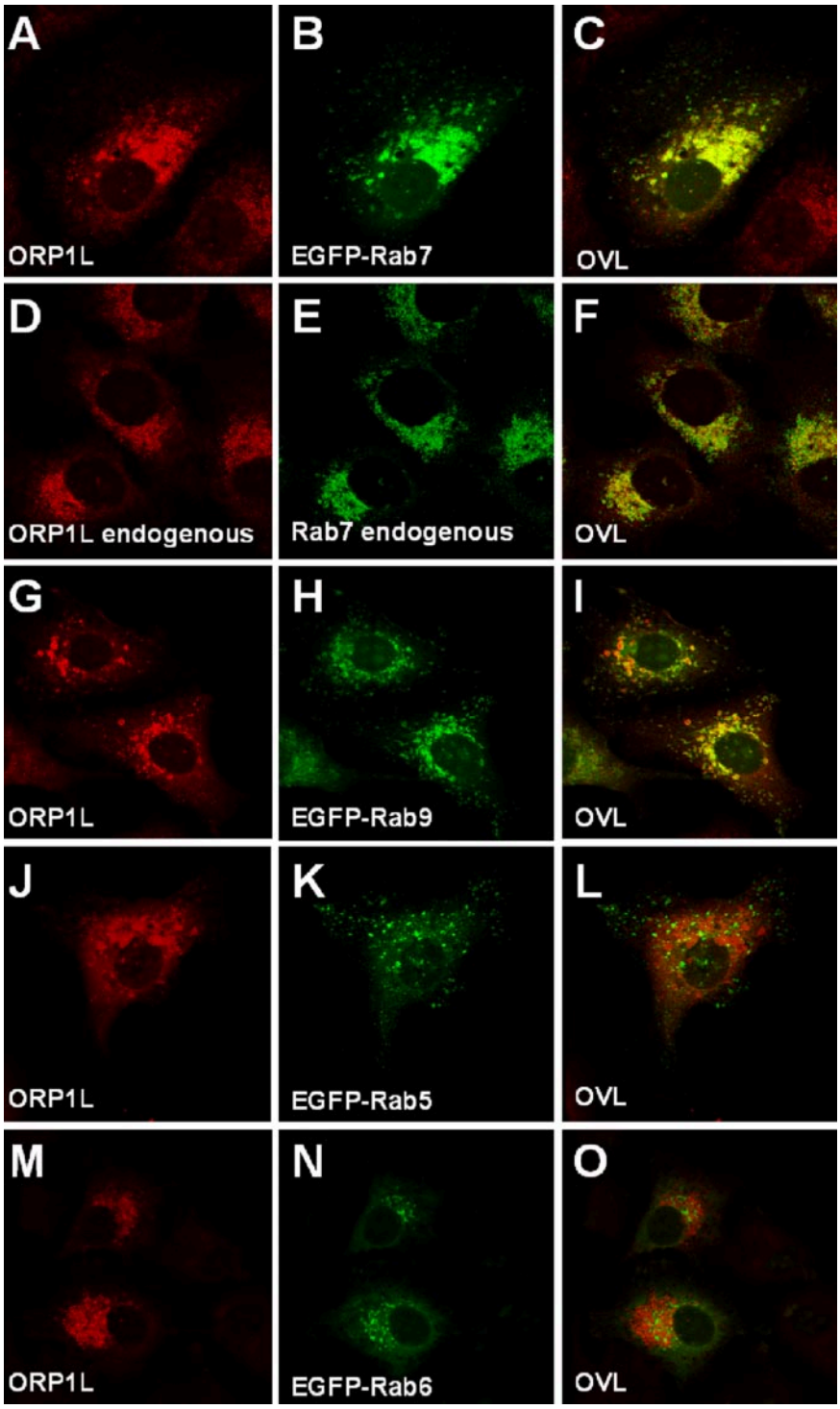

Figure 3. ORP1L colocalizes with the late endosomal GTPases Rab7 and Rab9 in HeLa cells. (A–C) Transfected cells overexpressing full-length human ORP1L and EGFP-Rab7. ORP1L was stained using specific rabbit (R247) antibodies, and the proteins were visualized by confocal microscopy. (D–F) Endogenous ORP1L and Rab7 stained with R247 and chicken anti-Rab7 antibodies, respectively. (G–I) ORP1L and EGFP-Rab9 coexpressed by double transfection. (J–L) ORP1L and EGFP-Rab5 coexpressed by double transfection. (M–O) ORP1L and EGFP-Rab6 coexpressed by double transfection. OVL, overlays.

To delineate which part of ORP1L binds Rab7, we carried out pull-down experiments using in vitro-translated, ^{35}S-labeled truncated fragments of ORP1L and GST-Rab7 that was immobilized on glutathione-Sepharose and loaded with the nonhydrolyzable GTP analog GTPγS. Full-length ORP1L, the N-terminal fragment containing the three ankyrin repeats (ANK, aa 1–237), and the fragment containing the PHD in addition to the ANK region (ANK+PHD, aa 1–408) were pulled down by GST-Rab7. The fragment comprising the PHD region and the C-terminal OSBP-related domain (PHD+ORD, aa 211–950) or the C-terminal ORP1S variant (aa 514–950) alone showed no affinity for Rab7 in the pull-down assay (Figure 6). These results provide a third piece of evidence for an interaction of ORP1L with Rab7 and demonstrate that the Rab7-binding determinant localizes within the N-terminal ankyrin repeat region (aa 1–237) of ORP1L.

ORP1L Stabilizes Rab7 on Late Endocytic Compartments

To assess the effects of ORP1L on the functional cycle of Rab7, we carried out FRAP experiments in HeLa cells trans-

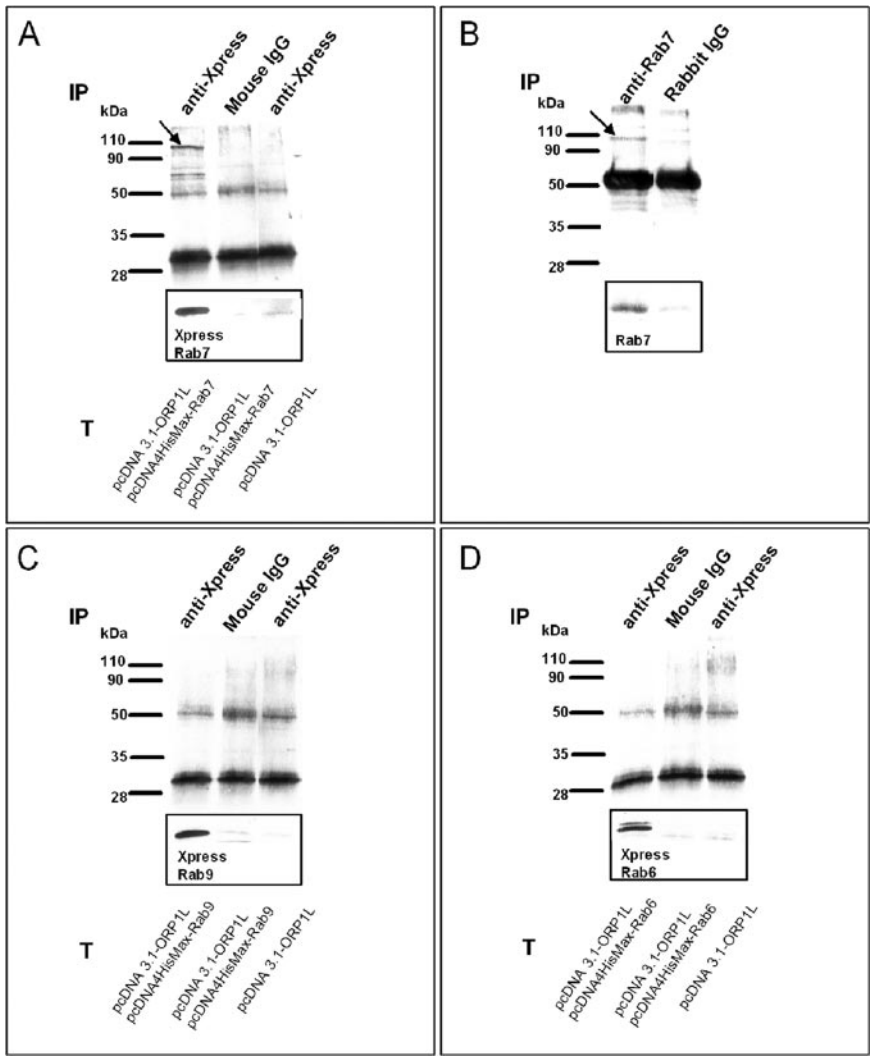

Figure 4. ORP1L coimmunoprecipitates with Rab7 in HeLa cells. (A) Transfected (T) cells overexpressing human ORP1L alone or together with Xpress epitope-tagged Rab7. ORP1L and Rab7 were immunoprecipitated (IP) with anti Xpress mAb or an irrelevant control mouse antibody. The precipitates were Western blotted with anti-ORP1L; the inset shows the corresponding lane blotted with Xpress antibody detecting epitope-tagged Rab7. The arrow indicates ORP1L. (B) Immunoprecipitation of endogenous proteins was carried out with rabbit anti-Rab7 or control antibodies. The arrow indicates ORP1L. (C) The same experiment as in A, with transfected cells overexpressing human ORP1L alone or together with Xpress epitope-tagged Rab9. (D) The same experiment as in A, with transfected cells overexpressing human ORP1L alone or together with Xpress epitope-tagged Rab6.

fected with EGFP-Rab7 in the presence or absence of ORP1L coexpression. Perinuclear clusters of EGFP-Rab7 containing endo/lysosomes were photobleached at 488 nm, and the recovery of fluorescence was monitored for 500 s. In cells cotransfected with the empty vector, a recovery curve reaching 65% of the starting fluorescence after 500 s was observed. In ORP1L-expressing cells, the recovery was markedly slower, ending up at a 32% recovery level after 500 s (Figure 7). This shows that ORP1L causes a prolonged residence of EGFP-Rab7 on the LE membranes and a consequent reduction in its rate of replacement by the unbleached GTPase, strongly suggesting that ORP1L stabilizes the GTP-bound active state of Rab7.

The ORP1L PHD Binds Phosphoinositides

A majority of the known pleckstrin homology domains show affinity for phosphoinositides, and in many cases, these domains function in targeting of proteins to membranes (Lemmon and Ferguson, 2000; Yu *et al*., 2004). We therefore assayed the interaction of the ORP1L PHD with phosphoinositides using a vesicle pull-down assay in which phosphatidylcholine (PC) vesicles containing 1 mol% of different phosphoinositides were incubated with glutathione-Sepharose containing either GST, GST-PHD(ORP1L), or GST-PHD(PLCδ) as a positive control. In this assay, the PLCδ PHD with high-affinity for phosphatidylinositol 4,5-bisphosphate [$PI(4,5)P_2$] (Varnai *et al*., 2002) pulled down ~20% of the $PI(4,5)P_2$-containing vesicles and also bound phosphatidylinositol 3,4-bisphosphate [$PI(3,4)P_2$] and phosphatidylinositol 3,4,5-trisphosphate weakly [$PI(3,4,5)P_3$]. The PHD of ORP1L interacted weakly with $PI(3,4)P_2$, phosphatidylinositol 3,5-bisphosphate, and $PI(3,4,5)P_3$, and binding was also detectable for phosphatidylinositol 3-monophosphate, phosphatidylinositol 4-monophosphate, and phosphatidylinositol 5-monophosphate (Figure 8). The results suggest that, like most PHDs, that of ORP1L does interact with phosphoinositides but with low specificity and affinity.

N-Terminal Fragments of ORP1L Cause Clustering of Lamp-1-positive Compartments

The effect of overexpression of the ORP1L N-terminal fragments that bind Rab7 on the morphology of Lamp-1-positive LEs/lysosomes was monitored by immunofluorescence microscopy. Expression of the ANK or ANK+PHD fragments caused a prominent effect on the LE/lysosome organization, resulting in strong clustering of the Lamp-1 compartments in the perinuclear region (Figure 9, A–F). Both of these

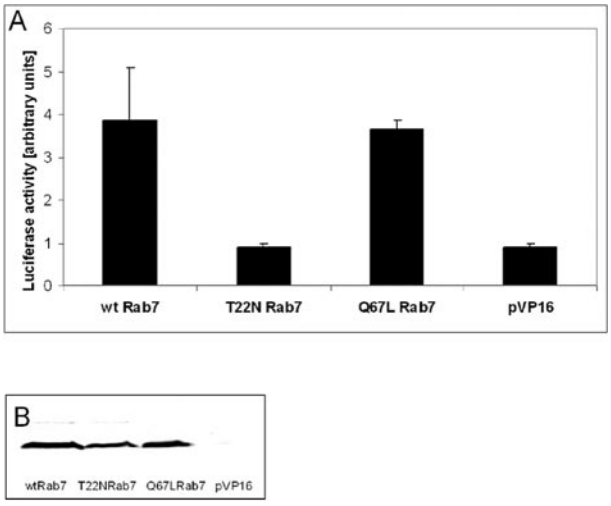

Figure 5. ORP1L interacts with Rab7-GTP in a COS cell two-hybrid assay. ORP1L in pM2 was transfected into COS cells together with wild-type Rab7, Rab7 Q67L, or Rab7 T22N (identified below the diagram) in pVP16, or the empty vector as a control (pVP16). The cells also received the pG5luc luciferase reporter plasmid and a β-galactosidase expression plasmid for normalization of values. (A) Mean luciferase activities ($\pm$SEM) of two experiments carried out in triplicate. (B) Similar expression levels of the activation domain fusions of wt Rab7 and the Q67L and T22N mutants. Equal amounts of cell lysate were Western blotted with anti-Rab7.

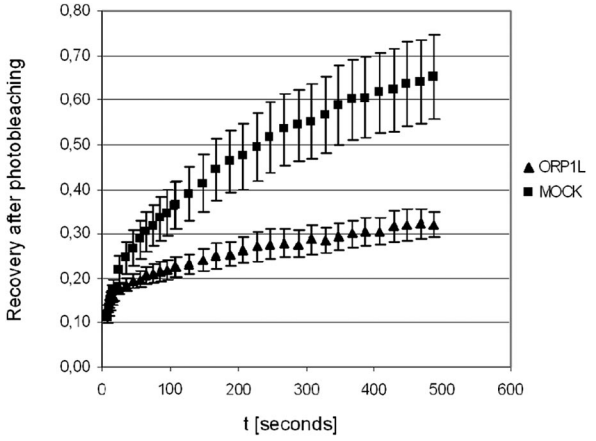

Figure 7. ORP1L mofidies the functional cycle of Rab7. HeLa cells grown on glass-bottomed dishes were transfected with EGFP-Rab7 together with the empty vector pcDNA4HisMax (MOCK) or the corresponding ORP1L expression vector (ORP1L). The GFP fluorescence of LE compartments was bleached, and fluorescence recovery (shown relative to the starting value, *y*-axis) as a function of time (*x*-axis) was recorded as detailed in *Materials and Methods*. The data displayed (mean $\pm$ SEM) represent five (MOCK) or four (ORP1L) recordings from different cells.

fragments seemed largely cytosolic, but they displayed some concentration on the Lamp-1-positive clusters, partially localizing on the surface of the LEs/lysosomes.

The overexpression of Rab7 or its constitutively active mutant has been reported to cause enlargement and perinuclear clustering of LE, whereas expression of the dominant inhibitory mutant T22N was shown to cause scattering of LE in the peripheral cytoplasm (Bucci *et al*., 2000). In double transfection experiments, expression of Rab7 T22N was found to reverse the perinuclear LE clustering caused by the ORP1L ANK or ANK+PHD fragment (shown for ANK+PHD in Figure 9, G–I). This indicates that active Rab7 may be required for the effects of the N-terminal ORP1L fragments on LE organization. Overexpression of the ORP1S protein variant lacking the N-terminal ANK and PHD regions had no effect on the LE organization (Figure 9, J–L).

ORP1L-induced Clustering of LEs/Lysosomes Requires Functional Dynein/Dynactin Motor Complexes

When the microtubule-dissociating agent nocodazole was added to cells overexpressing the ORP1L N-terminal fragments, large LE/lysosome clusters in the perinuclear region were absent (Figure 10, A–C), showing that the clustering effect is dependent on an intact microtubule cytoskeleton. It has been shown that overexpression of the dynactin subunit p50dynamitin disrupts the dynein/dynactin complex (Burkhardt *et al*., 1997; Valetti *et al*., 1999). When we overexpressed EGFP-p50dynamitin with ORP1L or the ANK or ANK+PHD fragments, the clustering effect was lost, and the ORP1-positive compartments were scattered throughout the cytoplasm (shown for ANK+PHD in Figure 10, D–F). Double immunostaining of overexpressed ORP1L or itsj fragments and endogenous p150^{glued} clearly showed that dynein/dynactin motor complexes were enriched on the ORP1-positive clustered compartments (shown for ANK+PHD in Figure 10, G–I), whereas such structures were absent in nonexpressing cells. These data demonstrate that the morphological effects of ORP1L on LEs/lysosomes are dependent on microtubules and that ORP1L facilitates recruitment of dynein/dynactin complexes to LEs/lysosomes, thereby enhancing minus-end-directed organelle movement.

Effects of ORP1L Overexpression on Endocytic Membrane Traffic

The effects of ORP1L expression on the endocytic process was investigated by internalizing TRITC-conjugated dextran

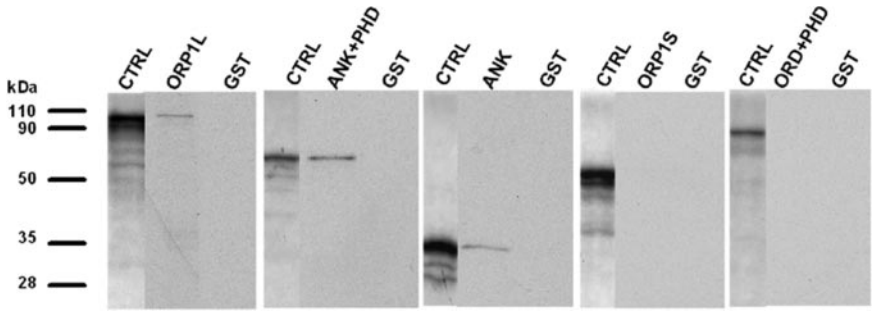

Figure 6. The Rab7 interaction determinant resides in the N-terminal ankyrin repeat region of ORP1L. Pull-down of in vitro-translated ^{35}S-labeled ORP1L, its truncated fragments, or the ORP1S variant was carried out using GST-Rab7 bound on glutathione-Sepharose and loaded with GTPγS, or plain GST as a negative control. The lanes labeled CTRL represent the in vitro-translated product (2 μl of translation mix loaded directly) from each construct.

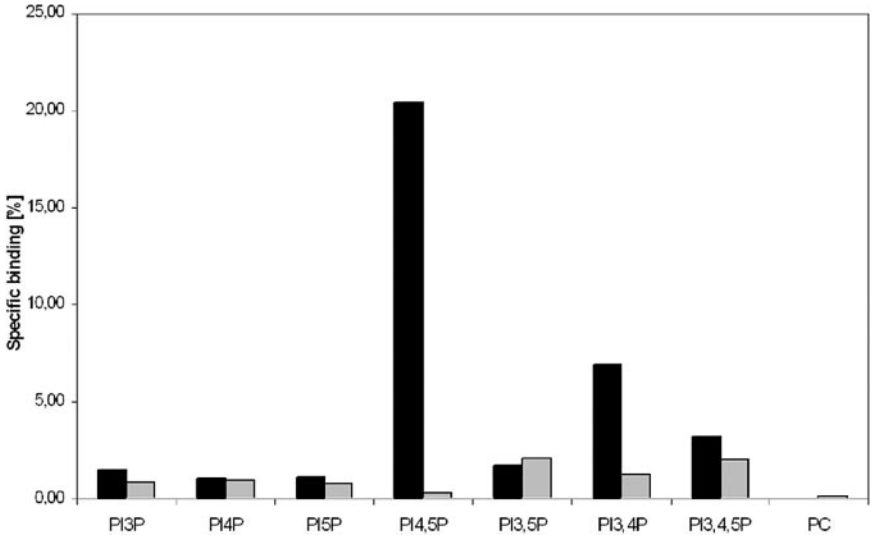

Figure 8. The PHD of ORP1L interacts with phosphoinositides. GST-ORP1L PHD fusion protein (gray bars) bound to glutathione-Sepharose beads was incubated with vesicles consisting of unlabeled PC, [^{14}C]PC, and 1 mol% of the indicated phosphoinositide. "PC" indicates binding to liposomes that consist of PC only. GST was used as a negative control (values subtracted from the results), and the PHD of PLCδ fused to GST (black bars) was used as a positive control. The lipid binding is expressed as a percentage of total radioactivity recovered. The data represents a mean from two independent experiments.

into transfected HeLa cells and monitoring the progression of the fluorescent dextran to Lamp-1-positive LEs/lysosomes as a function of time. After the 10-min uptake period, the internalized dextran was present in small endocytic structures that did not significantly colocalize with Lamp-1, both in cells expressing plain enhanced green fluorescent protein (EGFP) and in those expressing EGFP-ORP1L (Figure 11, A–H). In EGFP-expressing control cells, the dextran moved progressively to Lamp-1-positive late compartments during the chase, so that a major portion of the internalized marker reached these by 120 min (Figure 11, I–L). This movement was, however, disturbed in cells expressing EGFP-ORP1L. Even after the 120-min chase, the TRITC-dextran failed to reach those Lamp-1-positive compartments that had EGFP-ORP1L associated with their surface (Figure 11, M–P). Expression of EGFP-ORP1L was also found to cause a mild (32%) but significant inhibition of TRITC-dextran uptake during the 10-min internalization period compared with cells expressing plain EGFP (data not shown).

ORP1L Inhibits LE Vacuolation by H. pylori VacA

A hallmark activity of the *H. pylori* VacA protein is the formation of large cytoplasmic vacuoles of LE origin in mammalian cells upon treatment of the cells with weak bases (Papini *et al*., 2001; Montecucco and de Bernard, 2003). Prompted by the observed effects of ORP1L on the morphology and organization on LEs/lysosomes, we tested whether full-length ORP1L, the N-terminal ANK fragment, or the ANK+PHD fragment might have an impact on the vacuolation phenomenon caused by VacA. The LEs were visualized using EGFP-Rab7 (Li *et al*., 2004). The EGFP-Rab7-positive LEs displayed a normal morphology, and no vacuolization was observed when HeLa cells were cultured in presence of NH_4Cl only (Figure 12A). When VacA toxin was added, EGFP-Rab7 localized to large cytoplasmic vacuoles (Figure 12B). In specimens cotransfected with full-length ORP1L, cells in which the vacuole formation did not occur were frequently encountered. These cells often displayed clustering of Rab7 and ORP1L-positive endosomes in the perinuclear region (Figure 12, C and D). The inhibitory effect was clearly more pronounced in cells expressing the ANK or the ANK+PHD fragment (shown for the latter in Figure 12, E and F) than in cells expressing full-length ORP1L. Quantification of the effect revealed that vacuole formation occurred in 99% of the control cells expressing EGFP-Rab7 only, in 83% of cells expressing ORP1L, and in 60% of cells expressing ANK+PHD (Figure 12G). The inhibitory effect seemed to be dependent on the level of expression of ORP1L or ORP1L fragments; inhibition of VacA-induced vacuolation was increased in cells expressing high levels of these proteins.

DISCUSSION

In the present study, we show that in HeLa cells the OSBP homologue ORP1L localizes on late endocytic compartments and its distribution overlaps largely with those of Lamp-1, the small GTPase Rab7, a central regulator of late endosomal membrane trafficking events, and Rab9, a GTPase with a key role in the route from late endosomes to the *trans*-Golgi (Lombardi *et al*., 1993; Carroll *et al*., 2001). The finding that ORP1L overexpression induced clustering of LE/lysosomes prompted us to test whether ORP1L interacts with the late endosomal small GTPases. We show that both the endogenous and the overexpressed ORP1L and Rab7 proteins can be coimmunoprecipitated. The interaction seems to be specific for Rab7, because ORP1L does not coimmunoprecipitate with Rab9 or Rab6. Further evidence for the ORP1L–Rab7 interaction is provided by a COS cell two-hybrid assay, the results of which suggest that ORP1L preferably binds the active, GTP-bound form of Rab7. A third piece of evidence for a specific interaction between ORP1L and Rab7 is provided by an assay in which GST-Rab7 loaded with nonhydrolyzable GTPγS was capable of pulling down in vitro-translated ORP1L. This assay demonstrates that, of the truncated ORP1L fragments used, only ones that contain the N-terminal ANK repeat region, or the ANK region alone, bind Rab7-GTP, strongly suggesting that this region (aa residues 1–237) is sufficient for the Rab7 interaction. However, the present data do not indicate whether it is the ankyrin repeats themselves that specify this binding interaction.

The GTP-binding and hydrolysis cycle of Rab GTPases is connected with the dynamic localization of the proteins on specific membrane compartments (Zerial and McBride, 2001). Therefore, the GTP cycle can be indirectly monitored by observing the intracellular distribution of the protein using FRAP technology (Jordens *et al*., 2001). The FRAP

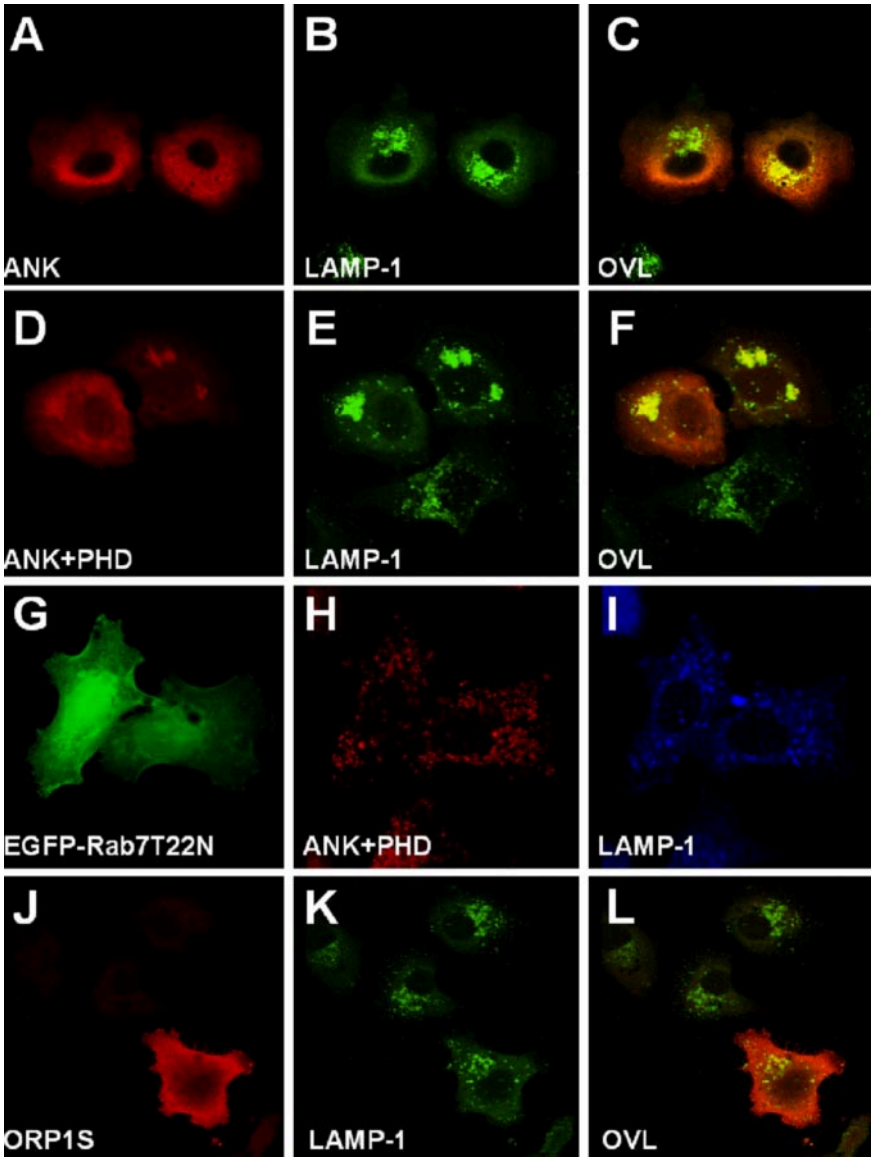

Figure 9. The N-terminal fragments of ORP1L cause clustering of Lamp-1 compartments. Xpress epitope-tagged ANK (aa 1–237) or ANK+PHD (aa 1–408) fragments of ORP1L were overexpressed in HeLa cells. The proteins were visualized with Xpress antibody, and late endocytic compartments were stained with anti-Lamp-1. (A–C) Expression of the ANK fragment. (D–F) Expression of the ANK+PHD fragment. (G–I) Coexpression of the ANK+PHD fragment with Rab7 T22N. (J–L) Expression of the ORP1S variant. OVL, overlays.

analysis of endo/lysosome-associated GFP-Rab7 revealed that ORP1L substantially slows down the rate at which membrane-bound bleached Rab7 is replaced by fluorescing GFP-Rab7. This suggests that ORP1L stabilizes active GTP-Rab7 on these compartments.

The PHD is immediately downstream of the ANK region of ORP1L. Using a vesicle pull-down assay, we show that this PHD binds several phosphoinositides with low affinity and specificity. The binding properties of ORP1L are thus similar to those of a majority of PHDs studied. Typically, additional interaction determinants or oligomerization of a PHD to increase avidity are necessary for efficient membrane targeting (Lemmon and Ferguson, 2000). The ANK region alone is capable of minimal LE targeting, consistent with the ability of this fragment to interact with Rab7. In HeLa cells, there is no significant difference in the localization of the ANK region and a fragment containing the ANK region and the PHD (ANK+PHD), so the role of the PHD in the LE targeting in this cell model remains unclear. However, in Chinese hamster ovary cells the ANK+PHD fragment showed clearly stronger LE targeting that the ANK region alone (Johansson *et al*., 2003), suggesting that the ANK region and the PHD may both play a role in the membrane association of ORP1L. In this respect, ORP1L could resemble another Rab binding partner, early endosomal antigen-1, which interacts with Rab5. This protein is recruited to early endosomes via interactions with both Rab5-GTP and phosphatidylinositol-3-phosphate (Simonsen *et al*., 1998; Gaullier *et al*., 2000).

The ANK and ANK+PHD fragments of ORP1L induce clustering of Lamp-1-positive LEs/lysosomes in the juxtanuclear region, but no obvious formation of enlarged Lamp-1 and Rab7-positive structures frequently observed with the full-length protein. Our recent findings show that the enlarged structures induced upon overexpression of the full-length protein in fact represent autophagic vacuoles (unpublished observations). Expression of the dominant inhibitory mutant T22N Rab7 counteracts the clustering phenotype induced by the ORP1L fragments. This mutant Rab7 was previously shown to cause dispersion of LEs (Bucci *et al*., 2000). The fact that Rab7 T22N reverses the LE clustering by ORP1L ANK and ANK+PHD indicates that this process

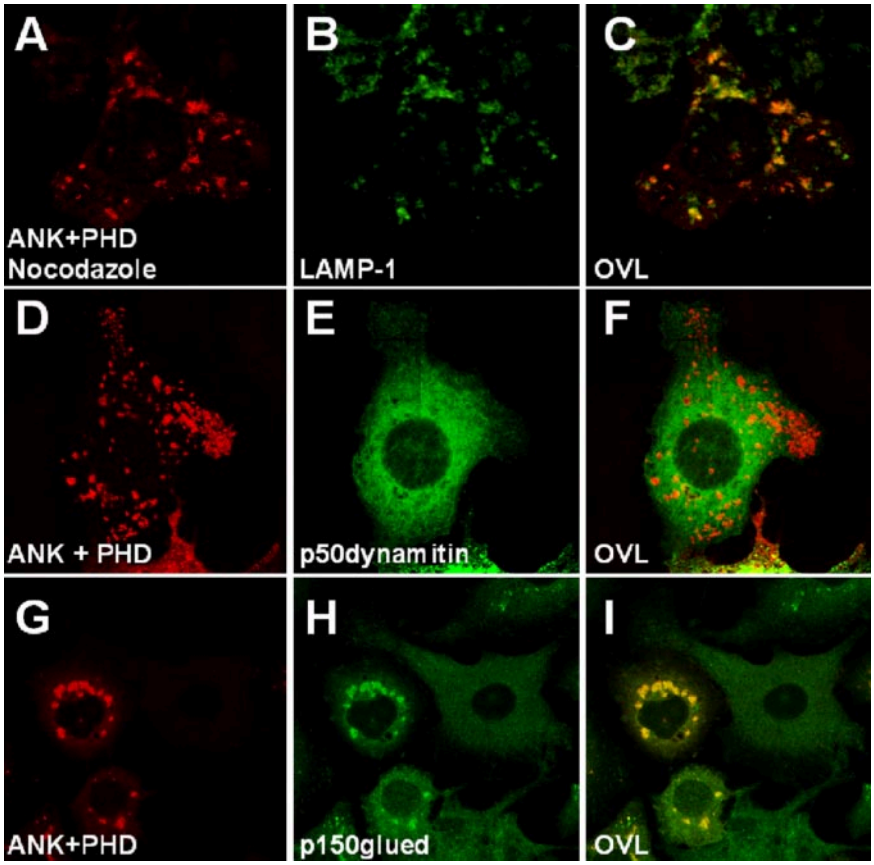

Figure 10. The clustering of LE by the ORP1L N-terminal fragment is dependent on microtubules and the dynein/dynactin motor complex. The ANK+PHD (aa 1–408) fragment of ORP1L was overexpressed in HeLa cells. (A–C) Cells were treated with 10 μM nocodazole for 30 min at 37°C before fixation. (D–F) Coexpression of the ANK+PHD fragment with EGFP-p50dynamitin. (G–I) Distribution of the endogenous p150^{glued} in cells expressing the ANK+PHD fragment.

requires active Rab7, in support of a functional interplay of ORP1L and the small GTPase. The LE/lysosomal localization of overexpressed ORP1L does not require simultaneous overexpression of Rab7, consistent with the notion that stoichiometric amounts of Rab7 are not necessary for membrane recruitment of ORP1L. This indicates that, even though ORP1L colocalizes extensively with Rab7 and interacts physically with the GTPase, its LE association involves other protein or lipid determinants in addition to Rab7.

The clusters induced by ORP1L or its N-terminal fragments are dissociated into smaller structures and dispersed throughout the cytoplasm when microtubules are destroyed using nocodazole. It has previously been demonstrated that the perinuclear localization of LEs/lysosomes as well as the transport of internalized proteins from early endosomes to LEs depends on microtubules (reviewed by Apodaca, 2001). The present finding is consistent with this and shows that, even though the clustering of LEs induced by ORP1L, ANK, and ANK+PHD is not fully reversed by microtubule dissociation, the large clusters in the juxtanuclear region are microtubule dependent. Other Rab7 binding partners identified so far include RILP, a protein that links Rab7-positive LEs to microtubule-dependent dynein/dynactin motor complexes and has strong effects on LE/lysosomal transport (Cantalupo *et al*., 2001; Jordens *et al*., 2001); Rabring7, which affects epidermal growth factor degradation and causes perinuclear aggregation of lysosomes (Mizuno *et al*., 2003); and the phosphatidylinositol 3′-kinase VPS34 and its adaptor protein p150 (Stein *et al*., 2003). The clustering of LEs/lysosomes induced by ORP1L and its ANK and ANK+PHD fragments resembles the effects of RILP or Rabring7 overexpression or that of Rab7 itself (Bucci *et al*., 2000). We show that the clustering effects of ORP1 are inhibited by overexpression of p50dynamitin, which uncouples the dynein motors from cargo (Burkhardt *et al*., 1997; Valetti *et al*., 1999) and that p150^{glued}, a component of the dynein/dynactin complex, is concentrated on ORP1-positive LEs/lysosomes. Recruitment of dynein/dynactin motor complexes to LE membranes is dependent on active GTP-Rab7 (Jordens *et al*., 2001). Therefore, our findings strongly suggest that interaction of ORP1L with GTP-Rab7 enhances recruitment of dynein/dynactin motor complexes to the endocytic compartments, which leads to enhanced minus-end-directed LE/lysosome movement.

In addition to the LE/lysosome clustering observed in cells expressing ORP1L, transport of the endocytosed marker TRITC-dextran to the late compartments with overexpressed EGFP-ORP1L on their surface was inhibited. Excessive engagement of Rab7 (and associated effectors) in abnormally abundant ORP1L interactions may significantly sequester these components, making them unavailable for their function in the tethering/docking/fusion of multivesicular bodies carrying incoming cargo from early compartments. Furthermore, excess ORP1L on endocytic compartments may sterically hinder normal vesicle interactions. Why EGFP-ORP1L also caused a mild inhibition of TRITC-dextran uptake is unclear. We did not see significant colocalization of the protein with an early endosomal marker, EGFP-Rab5, but there is a significant cytosolic fraction of ORP1L in transfected cells (Johansson *et al*., 2003), and this may interfere with components playing a role in early endocytic events.

H. pylori is a Gram-negative bacterium that inhabits the mucus of human gastric mucosa. This bacterium is a strong

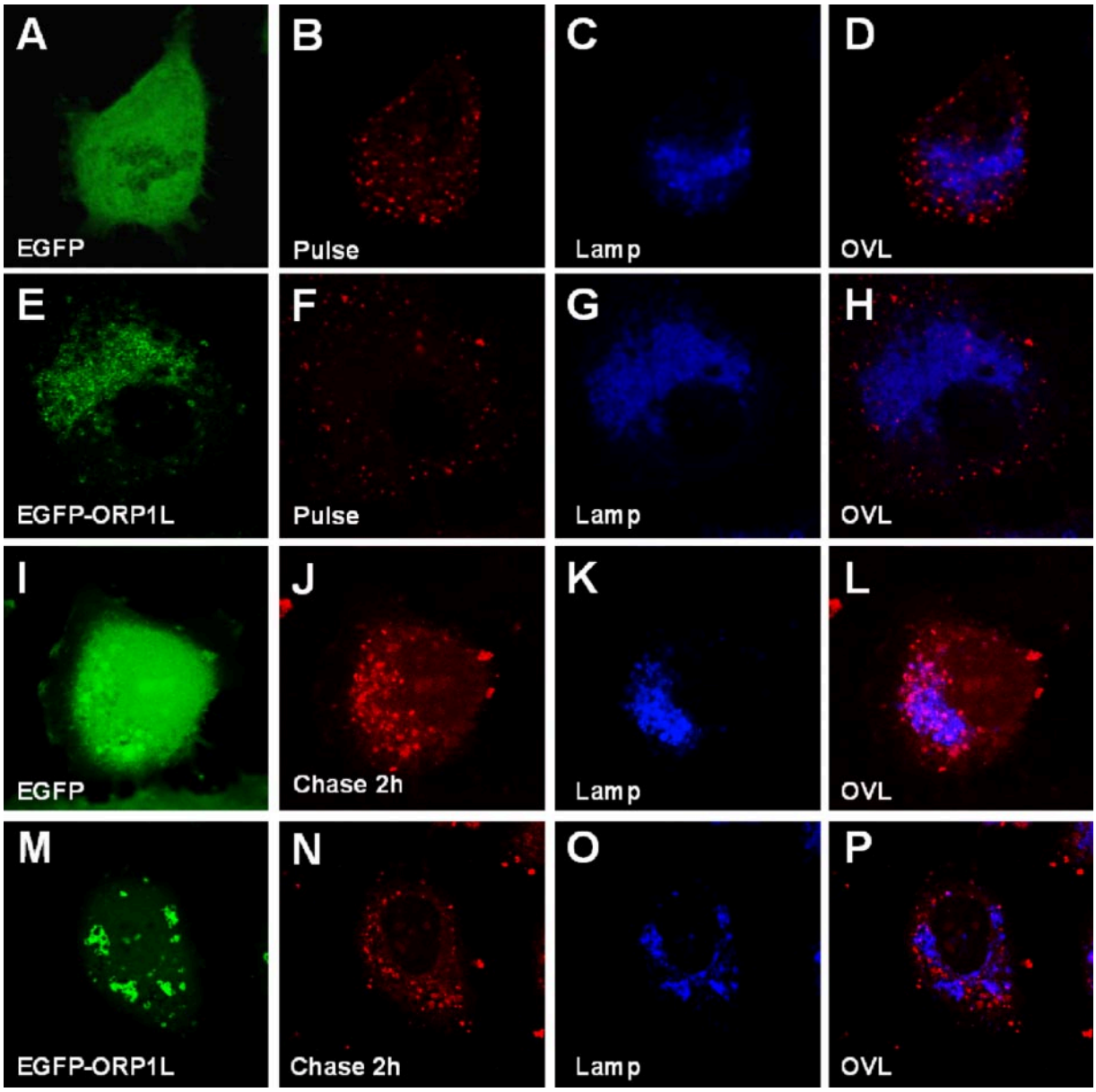

Figure 11. ORP1L overexpression disturbs endocytic membrane trafficking. TRITC-dextran was internalized for 10 min into HeLa cells transfected with EGFP or EGFP-ORP1L expression plasmids, followed by chase periods of up to 120 min. The cells were fixed and immunostained with anti-Lamp-1 mAb and viewed with a confocal microscope. (A–D) EGFP-expressing control cells fixed directly after the 10-min dextran uptake. (E–H) EGFP-ORP1L-expressing cells fixed directly after the 10-min uptake period. (I–L) EGFP-expressing control cells fixed after 120-min chase. (M–P) EGFP-ORP1L-expressing cells fixed after 120-min chase. D, H, L, and P are overlays illustrating the colocalization of the internalized TRITC-dextran with Lamp-1.

risk factor for the development of peptic ulcer disease and adenocarcinoma of the distal stomach (Dunn *et al*., 1997). Expression of the virulence factor VacA contributes to the capacity of *H. pylori* to colonize the gastric mucosa. A hallmark activity of the VacA protein is the formation of large cytoplasmic vacuoles of LE origin in mammalian cells upon treatment of the cells with weak bases (Papini *et al*., 2001; Montecucco and de Bernard, 2003). This process is inhibited by the dominant negative Rab7 mutant, indicating that it is dependent on the activity of Rab7 (Papini *et al*., 1997; Li *et al*., 2004). The vacuolation has been suggested to involve formation of anion-selective channels in LE membranes by VacA, resulting in anion influx and stimulation of proton pumping by the vacuolar ATPase. Protonated weak bases such as ammonium chloride accumulate in the endosomes and cause osmotic swelling (Papini *et al*., 2001; Li *et al*., 2004). We found that full-length ORP1L, but especially the ANK and ANK+PHD fragments, inhibited the vacuolization induced by VacA. The degree of inhibition seemed to correlate with the expression level of the ORP1L construct. Why would binding of ORP1 to GTP-bound Rab7 and the suggested stabilization of the GTP-bound Rab7 on membranes lead to inhibition of the vacuolization, a phenomenon dependent of active Rab7? Again, it is possible that excess ORP1L or the LE clustering induced by ORP1L or its N-terminal fragments renders the endosomal membranes abnormal in functional

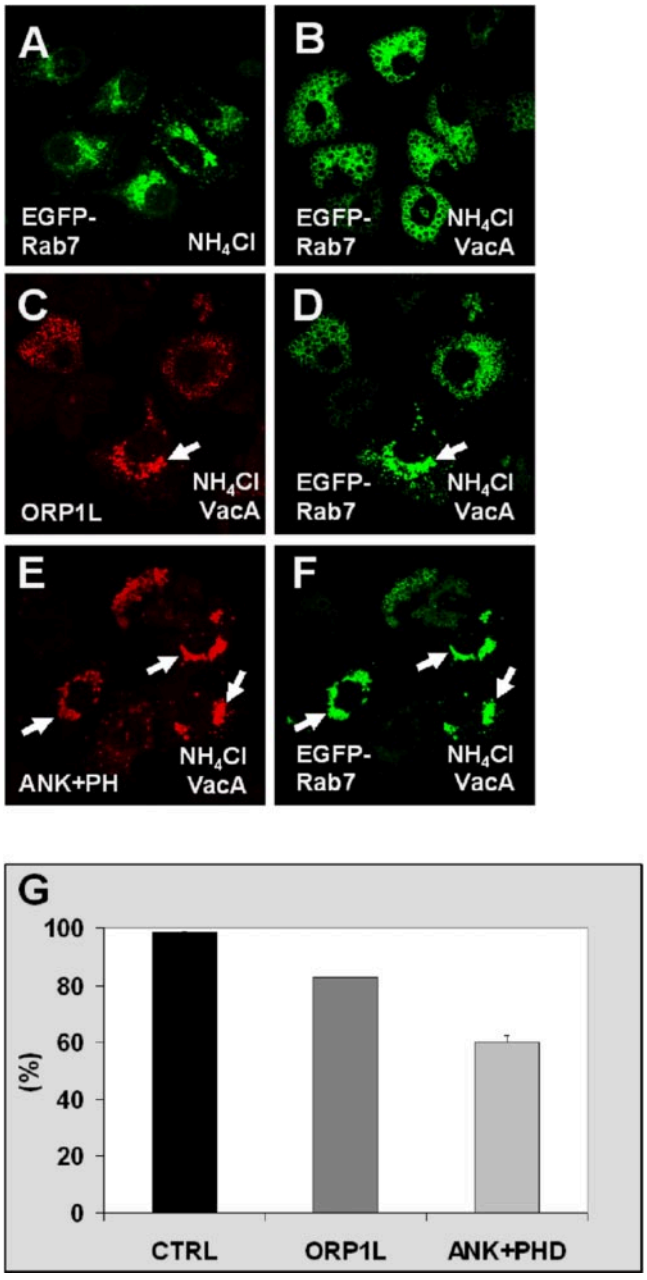

Figure 12. ORP1L overexpression partially inhibits vacuolation of HeLa cells induced by *H. pylori* VacA toxin. Cells were transfected with plasmids encoding human ORP1L or its N-terminal ANK+PHD fragment together with EGFP-Rab7. Vacuolation was induced by incubating the cells in medium containing *H. pylori* VacA and 5 mM NH_4Cl. The cells were stained with Xpress antibody. (A) Cells transfected with EGFP-Rab7 alone and incubation in the absence of VacA. (B) Cells transfected with EGFP-Rab7 alone and incubation with VacA. (C and D) Cells transfected with ORP1L and EGFP-Rab7, incubation with VacA. The arrow indicates a cell in which vacuolization has been inhibited. (E and F) Cells expressing the ANK+PHD fragment and EGFP-Rab7, and incubation with VacA. The arrows indicate cells in which vacuolation is inhibited. (G) Quantitation of the ORP1L effect on VacA-induced vacuolation. The bars show the percentage of transfected cells with vacuolar morphology of EGFP-Rab7-positive compartments. CTRL indicates cells transfected with empty vector and pEGFP-Rab7. The data represent means ± SEM from four independent transfections (120–160 cells were counted per coverslip).

properties required for VacA-induced cell vacuolation. This could, for example, involve incorporation of the VacA toxin or the function of the vacuolar proton ATPase in the LE membranes. One has to keep in mind that ORP1L may also affect the function of endocytic compartments via Rab7-independent mechanisms.

In summary, the present study identifies ORP1L as a novel interaction partner of Rab7 and demonstrates that overexpression of ORP1L or its truncated fragments modifies the organization and function of late endocytic compartments. This is the first report of a direct connection between the OSBP-related protein family and the master regulators of vesicle transport, the Rab GTPases.

ACKNOWLEDGMENTS

We are grateful to Seija Puomilahti and Pirjo Ranta for skillful technical assistance. Drs. Angela Wandinger-Ness, Marino Zerial, Tamas Balla, and Marije Marsman are thanked for kindly providing cDNA constructs. This study was supported by the Academy of Finland (Grant 51883 to M. L.; Grants 49987, 50641, 54301, and 206298 to V.M.O.), the Finnish Foundation for Cardiovascular Research (to V.M.O.), the Sigrid Juselius Foundation (to V.M.O.), and National Institutes of Health Grants R01 AI39657 and R01 DK53623 and the Department of Veterans Affairs (to T.L.C.). M. J. is member of the Helsinki Graduate School of Biotechnology and Molecular Biology.

REFERENCES

Apodaca, G. (2001). Endocytic traffic in polarized epithelial cells: role of the actin and microtubule cytoskeleton. Traffic *2*, 149–159.

Bishop, N. E. (2003). Dynamics of endosomal sorting. Int. Rev. Cytol. *232*, 1–57.

Bucci, C., Thomsen, P., Nicoziani, P., McCarthy, J., and van Deurs, B. (2000). Rab *7*, a key to lysosome biogenesis. Mol. Biol. Cell *11*, 467–480.

Burkhardt, J. K., Echeverri, C. J., Nilsson, T., and Vallee, R. B. (1997). Overexpression of the dynamitin (p50) subunit of the dynactin complex disrupts dynein-dependent maintenance of membrane organelle distribution. J. Cell Biol. *139*, 469–484.

Cantalupo, G., Alifano, P., Roberti, V., Bruni, C. B., and Bucci, C. (2001). Rab-interacting lysosomal protein (RILP): the Rab7 effector required for transport to lysosomes. EMBO J. *20*, 683–693.

Carroll, K. S., Hanna, J., Simon, I., Krise, J., Barbero, P., and Pfeffer, S. R. (2001). Role of Rab9 GTPase in facilitating receptor recruitment by TIP47. Science *292*, 1373–1376.

Chavrier, P., Parton, R. G., Hauri, H. P., Simons, K., and Zerial, M. (1990). Localization of low molecular weight GTP binding proteins to exocytic and endocytic compartments. Cell *62*, 317–329.

Choudhury, A., Dominguez, M., Puri, V., Sharma, D. K., Narita, K., Wheatley, C. L., Marks, D. L., and Pagano, R. E. (2002). Rab proteins mediate Golgi transport of caveola-internalized glycosphingolipids and correct lipid trafficking in Niemann-Pick C cells. J. Clin. Investig. *109*, 1541–1550.

Cover, T. L., Hanson, P. I., and Heuser, J. E. (1997). Acid-induced dissociation of VacA, the *Helicobacter pylori* vacuolating cytotoxin, reveals its pattern of assembly. J. Cell Biol. *138*, 759–769.

Dong, J., Chen, W., Welford, A., and Wandinger-Ness, A. (2004). The proteasome alpha-subunit XAPC7 interacts specifically with Rab7 and late endosomes. J. Biol. Chem. *279*, 21334–21342.

Dunn, B. E., Cohen, H., and Blaser, M. J. (1997). Helicobacter pylori. Clin. Microbiol. Rev. *10*, 720–741.

Edinger, A. L., Cinalli, R. M., and Thompson, C. B. (2003). Rab7 prevents growth factor-independent survival by inhibiting cell-autonomous nutrient transporter expression. Dev. Cell *5*, 571–582.

Feng, Y., Press, B., and Wandinger-Ness, A. (1995). Rab *7*, an important regulator of late endocytic membrane traffic. J. Cell Biol. *131*, 1435–1452.

Gaullier, J. M., Ronning, E., Gillooly, D. J., and Stenmark, H. (2000). Interaction of the EEA1 FYVE finger with phosphatidylinositol 3-phosphate and early endosomes. Role of conserved residues. J. Biol. Chem. *275*, 24595–24600.

Guignot, J., Caron, E., Beuzon, C., Bucci, C., Kagan, J., Roy, C., and Holden, D. W. (2004). Microtubule motors control membrane dynamics of *Salmonella*-containing vacuoles. J. Cell Sci. *117*, 1033–1045.

Gutierrez, M. G., Munafo, D. B., Beron, W., and Colombo, M. I. (2004). Rab7 is required for the normal progression of the autophagic pathway in mammalian cells. J. Cell Sci. *117*, 2687–2697.

Harrison, R. E., Brumell, J. H., Khandani, A., Bucci, C., Scott, C. C., Jiang, X., Finlay, B. B., and Grinstein, S. (2004). *Salmonella* impairs RILP recruitment to Rab7 during maturation of invasion vacuoles. Mol. Biol. Cell *15*, 3146–3154.

Harrison, R. E., Bucci, C., Vieira, O. V., Schroer, T. A., and Grinstein, S. (2003). Phagosomes fuse with late endosomes and/or lysosomes by extension of membrane protrusions along microtubules: role of Rab7 and RILP. Mol. Cell. Biol. *23*, 6494–6506.

Houlden, H., King, R. H., Muddle, J. R., Warner, T. T., Reilly, M. M., Orrell, R. W., and Ginsberg, L. (2004). A novel RAB7 mutation associated with ulcero-mutilating neuropathy. Ann. Neurol. *56*, 586–590.

Jager, S., Bucci, C., Tanida, I., Ueno, T., Kominami, E., Saftig, P., and Eskelinen, E. L. (2004). Role for Rab7 in maturation of late autophagic vacuoles. J. Cell Sci. *117*, 4837–4848.

Jaworski, C. J., Moreira, E., Li, A., Lee, R., and Rodriguez, I. R. (2001). A family of 12 human genes containing oxysterol-binding domains. Genomics *78*, 185–196.

Johansson, M., Bocher, V., Lehto, M., Chinetti, G., Kuismanen, E., Ehnholm, C., Staels, B., and Olkkonen, V. M. (2003). The two variants of oxysterol binding protein-related protein-1 display different tissue expression patterns, have different intracellular localization, and are functionally distinct. Mol. Biol. Cell *14*, 903–915.

Jordens, I., Fernandez-Borja, M., Marsman, M., Dusseljee, S., Janssen, L., Calafat, J., Janssen, H., Wubbolts, R., and Neefjes, J. (2001). The Rab7 effector protein RILP controls lysosomal transport by inducing the recruitment of dynein-dynactin motors. Curr. Biol. *11*, 1680–1685.

Lagace, T. A., Byers, D. M., Cook, H. W., and Ridgway, N. D. (1997). Altered regulation of cholesterol and cholesteryl ester synthesis in Chinese-hamster ovary cells overexpressing the oxysterol-binding protein is dependent on the pleckstrin homology domain. Biochem. J. *326*, 205–213.

Lagace, T. A., Byers, D. M., Cook, H. W., and Ridgway, N. D. (1999). CHO cells overexpressing the oxysterol binding protein (OSBP) display enhanced synthesis of sphingomyelin in response to 25-hydroxycholesterol. J. Lipid. Res. *40*, 109–116.

Lebrand, C., Corti, M., Goodson, H., Cosson, P., Cavalli, V., Mayran, N., Faure, J., and Gruenberg, J. (2002). Late endosome motility depends on lipids via the small GTPase Rab7. EMBO J. *21*, 1289–1300.

Lehto, M., Laitinen, S., Chinetti, G., Johansson, M., Ehnholm, C., Staels, B., Ikonen, E., and Olkkonen, V. M. (2001). The OSBP-related protein family in humans. J. Lipid Res. *42*, 1203–1213.

Lehto, M., and Olkkonen, V. M. (2003). The OSBP-related proteins: a novel protein family involved in vesicle transport, cellular lipid metabolism, and cell signalling. Biochim. Biophys. Acta *1631*, 1–11.

Lemmon, M. A., and Ferguson, K. M. (2000). Signal-dependent membrane targeting by pleckstrin homology (PH) domains. Biochem. J. 350, 1–18.

Levine, T. P., and Munro, S. (1998). The pleckstrin homology domain of oxysterol-binding protein recognises a determinant specific to Golgi membranes. Curr. Biol. *8*, 729–739.

Levine, T. P., and Munro, S. (2002). Targeting of Golgi-specific pleckstrin homology domains involves both PtdIns 4-kinase-dependent and -independent components. Curr. Biol. *12*, 695–704.

Li, Y., Wandinger-Ness, A., Goldenring, J. R., and Cover, T. L. (2004). Clustering and redistribution of late endocytic compartments in response to *Helicobacter pylori* vacuolating toxin. Mol. Biol. Cell *15*, 1946–1959.

Loewen, C. J., Roy, A., and Levine, T. P. (2003). A conserved ER targeting motif in three families of lipid binding proteins and in Opi1p binds VAP. EMBO J. *22*, 2025–2035.

Lombardi, D., Soldati, T., Riederer, M. A., Goda, Y., Zerial, M., and Pfeffer, S. R. (1993). Rab9 functions in transport between late endosomes and the trans-Golgi network. EMBO J. *12*, 677–682.

Marsman, M., Jordens, I., Kuijl, C., Janssen, L., and Neefjes, J. (2004). Dynein-mediated vesicle transport controls intracellular *Salmonella* replication. Mol. Biol. Cell *15*, 2954–2964.

Maxfield, F. R., and McGraw, T. E. (2004). Endocytic recycling. Nat. Rev. Mol. Cell Biol. *5*, 121–132.

Meresse, S., Gorvel, J. P., and Chavrier, P. (1995). The rab7 GTPase resides on a vesicular compartment connected to lysosomes. J. Cell Sci. *108*, 3349–3358.

Mizuno, K., Kitamura, A., and Sasaki, T. (2003). Rabring7, a novel Rab7 target protein with a RING finger motif. Mol. Biol. Cell *14*, 3741–3752.

Montecucco, C., and de Bernard, M. (2003). Molecular and cellular mechanisms of action of the vacuolating cytotoxin (VacA) and neutrophil-activating protein (HP-NAP) virulence factors of *Helicobacter pylori*. Microbes Infect. *5*, 715–721.

Ng Yan Hing, J. D., Desjardins, M., and Descoteaux, A. (2004). Proteomic analysis reveals a role for protein kinase C-alpha in phagosome maturation. Biochem. Biophys. Res. Commun. *319*, 810–816.

Papini, E., Satin, B., Bucci, C., de Bernard, M., Telford, J. L., Manetti, R., Rappuoli, R., Zerial, M., and Montecucco, C. (1997). The small GTP binding protein rab7 is essential for cellular vacuolation induced by *Helicobacter pylori* cytotoxin. EMBO J. *16*, 15–24.

Papini, E., Zoratti, M., and Cover, T. L. (2001). In search of the *Helicobacter pylori* VacA mechanism of action. Toxicon *39*, 1757–1767.

Pfeffer, S. R. (2001). Rab GTPases: specifying and deciphering organelle identity and function. Trends Cell Biol. *11*, 487–491.

Press, B., Feng, Y., Hoflack, B., and Wandinger-Ness, A. (1998). Mutant Rab7 causes the accumulation of cathepsin D and cation-independent mannose 6-phosphate receptor in an early endocytic compartment. J. Cell Biol. *140*, 1075–1089.

Schiavo, G., Gu, Q. M., Prestwich, G. D., Söllner, T. H., and Rothman, J. E. (1996). Calcium-dependent switching of the specificity of phosphoinositide binding to syntaptotagmin. Proc. Natl. Acad. Sci. USA *93*, 13327–13332.

Sedgwick, S. G., and Smerdon, S. J. (1999). The ankyrin repeat: a diversity of interactions on a common structural framework. Trends Biochem. Sci. *24*, 311–316.

Simonsen, A., Lippe, R., Christoforidis, S., Gaullier, J. M., Brech, A., Callaghan, J., Toh, B. H., Murphy, C., Zerial, M., and Stenmark, H. (1998). EEA1 links PI(3)K function to Rab5 regulation of endosome fusion. Nature *394*, 494–498.

Stein, M. P., Feng, Y., Cooper, K. L., Welford, A. M., and Wandinger-Ness, A. (2003). Human VPS34 and p150 are Rab7 interacting partners. Traffic *4*, 754–771.

Taylor, F. R., and Kandutsch, A. A. (1985). Oxysterol binding protein. Chem. Phys. Lipids *38*, 187–194.

Taylor, F. R., Saucier, S. E., Shown, E. P., Parish, E. J., and Kandutsch, A. A. (1984). Correlation between oxysterol binding to a cytosolic binding protein and potency in the repression of hydroxymethylglutaryl coenzyme A reductase. J. Biol. Chem. *259*, 12382–12387.

Valetti, C., Wetzel, D. M., Schrader, M., Hasbani, M. J., Gill, S. R., Kreis, T. E., and Schroer, T. A. (1999). Role of dynactin in endocytic traffic: effects of dynamitin overexpression and colocalization with CLIP-170. Mol. Biol. Cell *10*, 4107–4120.

Varnai, P., Lin, X., Lee, S. B., Tuymetova, G., Bondeva, T., Spat, A., Rhee, S. G., Hajnoczky, G., and Balla, T. (2002). Inositol lipid binding and membrane localization of isolated pleckstrin homology (PH) domains. Studies on the PH domains of phospholipase C delta 1 and p130. J. Biol. Chem. *277*, 27412–27422.

Verhoeven, K., *et al*. (2003). Mutations in the small GTP-ase late endosomal protein RAB7 cause Charcot-Marie-Tooth type 2B neuropathy. Am. J. Hum. Genet. *72*, 722–727.

Vieira, O. V., Bucci, C., Harrison, R. E., Trimble, W. S., Lanzetti, L., Gruenberg, J., Schreiber, A. D., Stahl, P. D., and Grinstein, S. (2003). Modulation of Rab5 and Rab7 recruitment to phagosomes by phosphatidylinositol 3-kinase. Mol. Cell Biol. *23*, 2501–2514.

Yu, J. W., Mendrola, J. M., Audhya, A., Singh, S., Keleti, D., DeWald, D. B., Murray, D., Emr, S. D., and Lemmon, M. A. (2004). Genome-wide analysis of membrane targeting by *S. cerevisiae* pleckstrin homology domains. Mol. Cell *13*, 677–688.

Zerial, M., and McBride, H. (2001). Rab proteins as membrane organizers. Nat. Rev. Mol. Cell Biol. *2*, 107–117.